Journal of Hazardous Materials 189 (2011) 278–285

Contents lists available at ScienceDirect

Journal of Hazardous Materials

journal homepage: www.elsevier.com/locate/jhazmat

Hydrothermal growth of free standing TiO_2 nanowire membranes for photocatalytic degradation of pharmaceuticals

Anming Hu[a,*], Xu Zhang[b], Ken D. Oakes[b], Peng Peng[a], Y. Norman Zhou[a], Mark R. Servos[b]

[a] Centre for Advanced Materials Joining, Department of Mechanical and Mechatronics Engineering, University of Waterloo, 200 University Avenue West, Waterloo, ON, N2L 3G1, Canada
[b] Department of Biology, University of Waterloo, 200 University Avenue West, Waterloo, ON, N2L 3G1, Canada

ARTICLE INFO

Article history:
Received 26 August 2010
Received in revised form 6 February 2011
Accepted 13 February 2011
Available online 19 February 2011

Keywords:
TiO_2 nanowire
Free standing membranes
Photocatalytic degradation
Pharmaceuticals
Microfiltration

ABSTRACT

Highly entangled TiO_2 nanowires were directly synthesized by hydrothermal growth on Ti substrates at 180 °C utilizing various organic solvents to oxidize Ti. The growth mechanism, microstructure and phase transition of TiO_2 nanowire membranes were investigated in detail. TiO_2 nanowires, with diameters of 10–20 nm and lengths up to 100 μm, show a phase transition from Type-B to anatase by annealing at 700 °C. Robust, free standing TiO_2 nanowire membranes with millimeter level thickness can be cleaved from Ti substrates or directly prepared from thin Ti foils. These porous TiO_2 membranes, while effective for mechanical microfiltration, can also photocatalytically degrade pharmaceuticals such as trimethoprim under UV irradiation.

1. Introduction

Pharmaceuticals and personal care products (PPCPs) are considered emerging contaminants of concern as their incomplete removal during municipal wastewater treatment has resulted in the frequent detection of these chemicals in surface and ground water around the globe [1,2]. Typical drinking water treatment systems are only partially capable of removing this diverse group of chemicals from contaminated water sources, and their occurrence in drinking water has been recently widely reported [1–3]. The cost-effective removal of PPCPs and other organic contaminants from wastewater and drinking water remains a challenge [4]. Use of micro/ultra membrane filtration is also only partially effective for removal of these chemicals [5]. Nanofiltration is more effective but the fouling by organic matter, found in most surface water supplies, limits the application of this technology to relatively clean sources [6,7].

There has recently been a dramatic increase in TiO_2 materials' research, spanning disciplines as diverse as photovoltaics, sunscreens, chemical/gas sensors, commercial pigments, and their use for photocatalytic degradation of harmful organic materials in air and water [8–11]. With respect to the latter application, under UV excitation, TiO_2 generates electron–hole pairs which migrate separately to the materials' surface to form strong oxidative species such as hydroxyl radicals. These oxidative species are extremely efficient at mineralizing most organic contaminants, thereby eliminating sludge production and bio-fouling problems inherent to traditional micro/ultra filtration approaches. TiO_2 nanomaterials have demonstrated their potential as a viable, alternative drinking water treatment by effectively degrading a variety of emerging and traditional waterborne environmental pollutants including organic molecules, PPCPs and bacteria [7–14]. Recently, the multifunctional nature of TiO_2 nanowire/nanotube membranes in concurrently providing mechanical filtration and photocatalytic degradation of organic pollutants has been demonstrated [13–15].

Currently, there are multiple approaches to producing and refining TiO_2 materials using various substrates, oxidizing agents, and thermal environments. Hydrothermal growth of gram level TiO_2 nanowires using TiO_2 powder in a 5–10 M alkali solution has been extensively employed [16]. However, TiO_2 nanowires synthesized in this manner form dense, opaque bulks requiring further crushing and grinding prior to deposition into TiO_2 membranes. This is problematic as TiO_2 nanowires are relatively fragile, and processes requiring grinding shorten the TiO_2 nanowires, ultimately lowering the mechanical filtration performance of resulting membranes. Conversely, macroporous TiO_2 nanobar films, with a thickness of a few micrometers, have been synthesized on Ti substrates using acetone to oxidize Ti at 850 °C [17,18]. However, these films are

* Corresponding author.
E-mail address: a2hu@uwaterloo.ca (A. Hu).

0304-3894/$ – see front matter © 2011 Elsevier B.V. All rights reserved.
doi:10.1016/j.jhazmat.2011.02.033

too thin, and the processing temperatures too high for large-scale applications. In 1 M NaOH solution, TiO_2 nanowire films with a thickness of a couple of micrometers can be grown hydrothermally at 230 °C for use as a photo-anode of dye-sensitized solar cells [19,20]. At relatively low temperatures, Wu et al. [21] used hydrogen peroxide to directly oxidize Ti at 80 °C. Oriented titania nanorod films with a thickness of a few micrometers can be produced on the surface of Ti foils, which after calcination at 450 °C, can be converted to a mixture of anatase and rutile phases. Utilizing hydrothermal growth in a 10 M NaOH and 35% (w/v) H_2O_2 solution at 220 °C, $Na_2Ti_2O_4(OH)_2$ nanotube films of a few micrometers thickness can be synthesized on Ti substrates and transformed into TiO_2 nanowires after ion exchanging and calcinations [22,23]. This approach has been further optimized by Wu et al. [24] whereby porous TiO_2 nanowire films of a few micrometers can be fabricated on Ti substrates at 80 °C. Although these thick titania films display effective photocatalytic applications [21–24], they are too thin and mechanically fragile to serve as free-standing membranes.

In the present study, we directly grow dense TiO_2 nanowire membranes on Ti substrates at 180 °C within a 10 M NaOH solution utilizing various organic oxidizing solvents such as acetone, formamide, formic hydrazide, acetamide, and monoethanolamide. With the exception of acetone, which limits the growth of TiO_2 nanowires to a few micrometers in length, these solvents resulted in the growth of entangled TiO_2 nanowires with lengths up to 100 μm. This allowed us to prepare high performance TiO_2 nanowire membranes with millimeter level thickness for an evaluation of their application for microfiltration and photocatalytic degradation of several common PPCP contaminants.

2. Experimental

TiO_2 nanowires were synthesized on 99.99% pure titanium foil plates (20 mm × 20 mm of 0.25 or 0.127 mm thickness) pre-cleaned in an ultrasonic acetone bath (10 min), followed by an ultrapure water (resistivity 18 MΩ cm) rinse for an additional 10 min interval. Hydrothermal growth was carried out in a 125 mL Teflon-lined autoclave with 60 mL of 10 M NaOH solution. Various organic solvents including acetone, formamide, formic hydrazide, acetamide, and monoethanolamide were added as 5% (v/v) oxidizing solutions. For comparison, TiO_2 growth in solutions containing only basic alkaline or only organic solvents was also investigated. The reaction temperature and processing time were 160 °C or 180 °C and 3 days, respectively. After the reaction was complete, the autoclave was naturally cooled to room temperature, and both sides of each Ti foil plate were covered by white cotton-like membranes. These membranes were washed with ultrapure water before immersion in 0.02 M hydrochloric acid for 8 h. Subsequently the membranes were again washed in ultrapure water until the pH value of the water solution became neutral. The membranes were then dried at 100 °C for 2 h prior to their separation from the Ti foil plates with the help of a shaving knife. A thin Ti foil with a thickness of 0.127 mm was completely converted into a bilayer membrane (without Ti remaining). Tube-shaped membranes were prepared by rolling Ti foils. Phase transition of these titanate membranes was studied after annealing at elevated temperatures in air.

Microstructure and phase identification of titanate membranes were investigated with scanning electron microscopy (SEM), X-ray diffractometry (XRD) and transmission electron microscopy (TEM). TEM samples were prepared by dispersing TiO_2 nanowires in ethanol and then dripping aliquots onto a lacey carbon support film composed of a Cu grid. Diffuse reflectance spectra were measured by a UV–NIR spectrometer with an integrated spherical detector using $BaTiO_3$ as reference material.

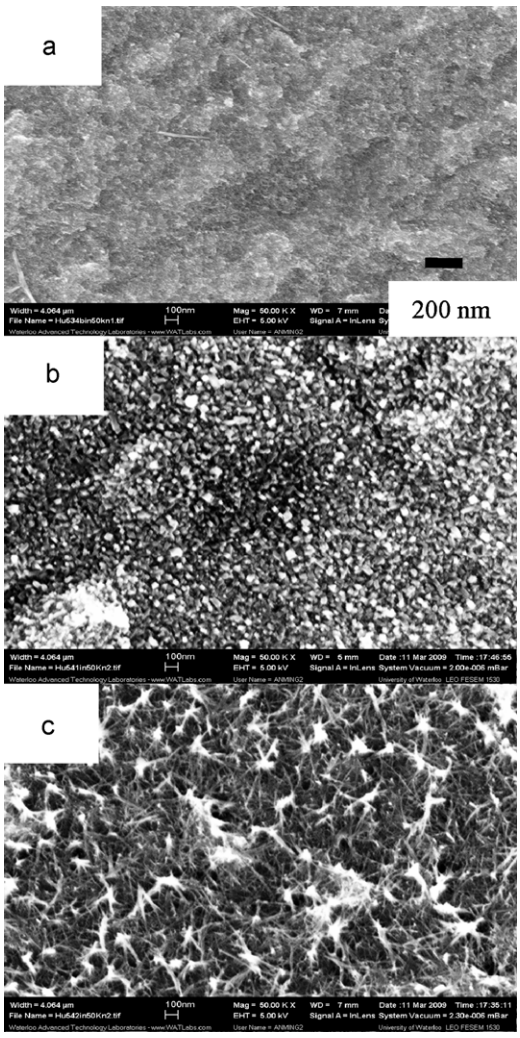

Fig. 1. Typical SEM images of Ti surfaces in (a) 10 M NaOH solution alone, (b) anhydrous acetone alone, and (c) 10 M NaOH solution with acetone. Scale is the same for all three panels.

The porosity of TiO_2 nanowire membranes was measured by the BET method (Quantachrome Instruments NOVA 2200) using nitrogen gas for adsorption. The permeability of TiO_2 nanowire membranes was characterized using a polycrystalline diamond suspension and a silver nanoparticle solution. The diamond solution was prepared by spraying commercial grinding paste (mean size 250 nm) into ultrapure water. Silver nanoparticle solution (1 mM) was generated from reduced $AgNO_3$ by sodium citrate at 90 °C with the addition of poly(vinyl pyrrolidone) (PVP). The concentration of diamond particles was determined by UV–vis absorption spectra relative to calibration curves of known concentration. The permeability measurement was carried out using a funnel with a porous glass to support the TiO_2 nanowire membranes or filter paper (Whatman™ # 1001042). A slight vacuum (about 5% lower than standard ambient pressure) was applied to the sealed flasks to speed up the filtration. Photocatalytic degradation assessments were evaluated on a suite of 13 pharmaceuticals (including norfluoxetine, lincomycin, sulfamethoxazole, diclofenac, trimethoprim, bisphenol A, fluoxetine, venlafaxin, gemfibrozil, atrazine, carbamazepine, ibuprofen, and atorvastatin), each at a concentration of approximately 100 μg/L (in ultrapure water). The persistence of analytes in treatments with and without TiO_2 membranes, and in the presence and absence of 100 W UV irradiation, was evaluated to elucidate degradation efficacy and

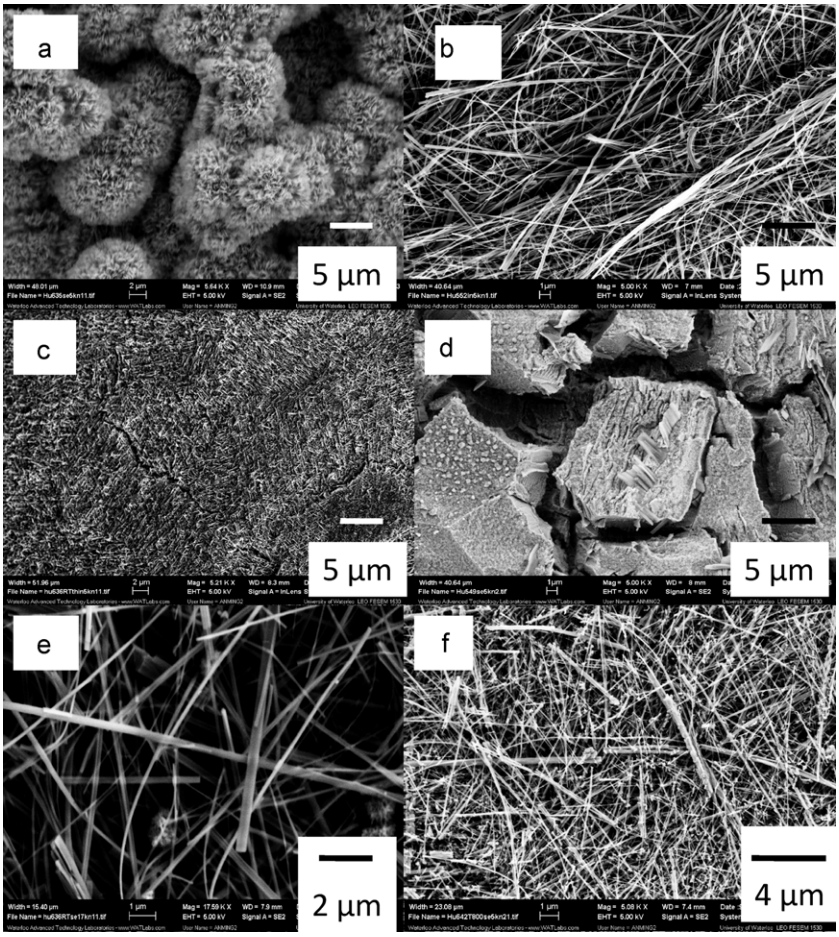

Fig. 2. Growth morphology of TiO_2 membranes at (a) 160 °C and (b) 180 °C with acetamide as the oxygen source. Removal of white-pulp-like surface layers reveals (c) an indigo surface of Ti substrates and (d) a densified layer between the indigo surface and white top membranes. TiO_2 nanowire membranes calcined (e) at 700 °C for 2 h and (f) at 800 °C for 2 h.

the influence of nanowire UV irradiation and surface absorption. Assessments of photocatalytic degradation were carried out within aqueous solutions at room temperature (around 22 °C) with a pH value of 6.7 employing 100 mg of TiO_2 membranes in 80 mL ultrapure water. For comparison, a commercially available TiO_2 anatase powder (Degussa P25, BET area, ca. 50 m^2/g; TEM particle size, 20–30 nm), also at a concentration of 100 mg in 80 mL water. The low pressure mercury UV lamp was kept 5 cm above the solution in order to avoid any thermal influences, and the irradiation intensity was 2.7×10^{-4} W/cm^2 recorded by a radiometer (International Light, IL 1700, Harvard) at the same distance. TiO_2 membranes were stable for these photocatalytic experiments, with neither remarkable microstructure nor phase change occurring, before or after experiments, as confirmed by both XRD and SEM characterizations.

To avoid introduction of nanomaterials into the instrument, a solid-phase microextraction (SPME) technique was employed for the cleanup of the samples treated by the nanowire based membrane. The samples were centrifuged for 20 min at 15 000 rpm, and each supernatant was transferred to duplicate 1.5 mL amber vials for the SPME extraction, calibrated by standard addition to compensate for potential matrix effects. Polydimethylsiloxane (PDMS) fibers were used as the extraction phase, with 15 h of extraction time utilized to ensure equilibrium. The extracted pharmaceuticals were desorption into 100 μL of methanol solution containing 7.5 ng/mL of lorazepam as an injection standard to calibrate for variations in injection volume by the HPLC. The instrumental separation and quantification were performed by HPLC–MS/MS (Agilent 1100 LC and AB Sciex 3200 QTrap). Identification and quantification of trimethoprim and other PPCPs were performed by comparing primary and secondary transitions against intensities of standard spectra of known concentrations with errors minimized by measuring samples in triplicate, as described in detail previously [25].

3. Results and discussion

3.1. Microstructure characterization

Comparative nanowire growth on Ti foils after 72 h in NaOH alone, acetone alone, and NaOH with acetone is shown in Fig. 1. A dense film with dispersive nanoparticles and sparse nanowires growth resulted from the 10 M NaOH solution alone treated at 180 °C (Fig. 1(a)); while some nano-rods with an average length in the tens of nanometer range were formed using 2 mL of pure acetone (Fig. 1(b)); whereas entangled nanowires of a few micrometers in length were synthesized in the presence of 10 M NaOH with 5% acetone (Fig. 1(c)). Although not shown in this paper, XRD patterns demonstrated that the resulting nanorods are pure TiO_2 while the film and nanowires are sodium titanate. Although these results can be understood in the context of similar growth mechanisms discussed in previous experiments [17–24], current nanowires are fabricated by a more facile process. Hydrothermal growth dramatically decreases the required processing temperature from 850 °C [17,18] to 180 °C through the use of acetone as the oxygen source for Ti oxidation. A more alkaline environment also reduces the

required processing temperature, with 10 M NaOH adequate for the growth of titanate nanowires at 180 °C while a reaction temperature of 230 °C is required if 1 M NaOH is used [19,20]. Notably, there is little titanate nanowire growth in 10 M NaOH at 180 °C without acetone, indicating the initial oxidization step is important and the formation of TiO_2 facilitates the growth of titanate nanowires. Due to insufficient oxidative radicals in NaOH solution, the growth of titania nanowires is not favoured on Ti foils. Hence, both the higher concentrations of alkaline solution and acetone as the oxygen source are required for the formation of titanate nanowires.

We investigated other organic solvents as alternative oxygen sources to optimize the growth of titania nanowires. Fig. 2 illustrates the growth morphology at 160 °C (Fig. 2(a)) and 180 °C (Fig. 2(b)) after 72 h when acetone is replaced by 5% acetamide. Obviously, both processing temperatures and solvents have a significant effect on the final structure of titania films. A lower temperature of 160 °C leads to the growth of a flower-shaped structure with petals composed of curved titania sheets only a few nanometer in thickness. Copious amounts of tweed nanowires are grown at 180 °C, each with diameters of 10–15 nm and lengths up to 100 μm. Similar growth to that illustrated can be obtained by replacing acetamide with formamide, formic hydrazide or monoethanolamide. As comparable growth of TiO_2 nanowires is obtained with any of these oxidizing solvents, it appears the common carbonyl groups in these compounds are providing the oxygen source for Ti oxidization. However, the substitution of acetone leads to the synthesis of longer titania nanowires compared to the results shown in Fig. 1. However, acetamide appears to be the best oxidant choice since significant amounts of TiO_2 nanoparticles are also synthesized when using other organic solvents as oxidants.

To elucidate the details of the nanowire growth mechanism, we removed the white pulp-like nanowires on the uppermost layer of the membrane until a dense, thin white layer appeared, the textured nanoribbon morphology of which is shown in Fig. 2(c). Digging deeper and removing this dense thin layer, the Ti foil reveals a slight indigo color. The microstructure of this indigo layer appears like grainy islands of approximately 10 μm size interspersed with irregular cracks (Fig. 2(d)). Detailed structural examination revealed the grains are assembled from multiple thin layers. These grains are likely formed by broken films arising from the differential thermal expansion coefficients of the surface film and metallic substrate. The post-annealing processes do not dramatically change the morphology of the titanate nanowires, as they remain stable after treating at 700 °C for 2 h (Fig. 2(e)). However, annealing at 800 °C (shown in Fig. 2(f)) leads to partial melting of the titanate nanowires, with thinner nanowires changing into a chain shape associated with some spherical nanoparticles.

3.2. Phase transition and growth mechanism

XRD patterns of titanate nanowires after annealing at elevated temperatures are shown in Fig. 3. The dominant diffraction peaks can be indexed on a $H_2Ti_3O_7$ structure (JCPDS 41-0192) for washed titanate nanowires, TiO_2-B (JCPDS 46-1238) for annealed nanowires at 400–500 °C, and anatase phase (JCPDS 21-1272) after annealing at 700 °C. Two small peaks added at approximately 22° and 43° correspond to TiO_2-B phase, indicating the governed phase of titanate nanowires annealed at 700 °C is dominantly anatase (denoted as A), with a minor amount of TiO_2-B phase (denoted as B on Fig. 3) as is consistent with numerous other studies [24,26–29]. It is well accepted that during hydrothermal reactions, Ti–O–Ti bonds of TiO_2 are broken and Ti–O–Na and Ti–O–H are formed, leading to the growth of $(Na,H)_2Ti_3O_7$ nanowires [26,27,29]. Utilizing ion exchange through washes in water and diluted HCl, Na^+ is eventually replaced by H^+. TiO_2-B phase is formed by dehydration

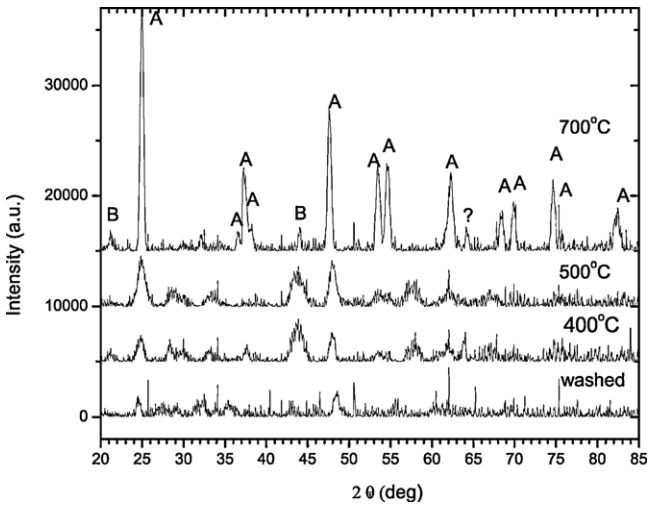

Fig. 3. XRD patterns of TiO_2 nanowire membranes with washing in water and diluted HCl and calcined at different temperatures. A: Anatase phase and B: TiO_2-B phase. ?: unidentified phase.

during annealing at 200–500 °C [26–29]. After elevated temperature annealing over 600 °C, TiO_2-B is converted into TiO_2 anatase phase, as was confirmed by high resolution TEM observations.

Typical TEM images demonstrating that the synthesized titanate nanowires are crystalline are found in Fig. 4. A lattice fringe of titanate nanowires without annealing corresponds to a d-spacing of 0.20 nm, which is consistent with the spacing of (2 0 4) planes of $H_2Ti_3O_7$. For annealing at 700 °C, nanowires displayed near single crystalline structure with a fringe spacing of 0.352 nm, corresponding to the spacing of (1 0 1) planes of TiO_2 anatase phase [23,30]. For annealing at 400 °C and 500 °C, most of the area shows a spacing of 0.36 nm, which corresponds well to (1 1 0) lattice planes of TiO_2-B. It is apparent there are different crystalline orientations when annealing at intermediate temperatures. These areas of differing orientation form small grains (3–5 nm in diameter, larger when annealed at 500 °C than at 300 °C) which supports the oriented attachment growth [29,31]. Associated with the crystalline growth of TiO_2-B from the hydrogen titanate phase, the small TiO_2-B grains rotate and re-arrange themselves with eliminating dislocations. The further phase transition from TiO_2-B to anatase leads to the synthesis of single crystalline TiO_2 anatase nanowires.

A schematic diagram of the formation of TiO_2 membranes on Ti substrates is illustrated in Fig. 5(a). In the initial reaction, a TiO_2 layer is formed on the surface of Ti due to oxidization. Using the hydrothermal process, the carbonyl group of one of the numerous potential oxidizing solvents provides the oxygen source. Subsequently, the oriented titanate nanosheets grow on the surface of the TiO_2 grains by the continuing diffusion of Ti cations through the network of TiO_2 grain boundaries [17]. These oriented nanosheets should be layered $Na_2Ti_3O_7$, as confirmed by their conversion into $H_2Ti_3O_7$ following ion exchange of Na^+ for H^+ [32]. These $Na_2Ti_3O_7$ nanosheets do not block the diffusion of the Ti cation, allowing the growth of membranes assembled by $(Na,H)_2Ti_3O_7$ nanowires on top of these nanosheets. It is important to point out that these nanowires are not formed during the water and diluted HCl treatments as the tweed nanowires are confirmed by SEM observation prior to washing (Fig. 5(b)). Due to different thermomechanical properties between Ti substrates and grown layers, the top-layer membranes can be easily cleaved from Ti substrates. A square-shaped TiO_2 nanowire membrane (2.5 cm^2; 0.5 mm thick) is shown in Fig. 5(c). Fig. 5(d) is a tube-shaped TiO_2 membrane with a diameter of 2.5 cm and length of 5 cm converted from a rolled Ti foil. To

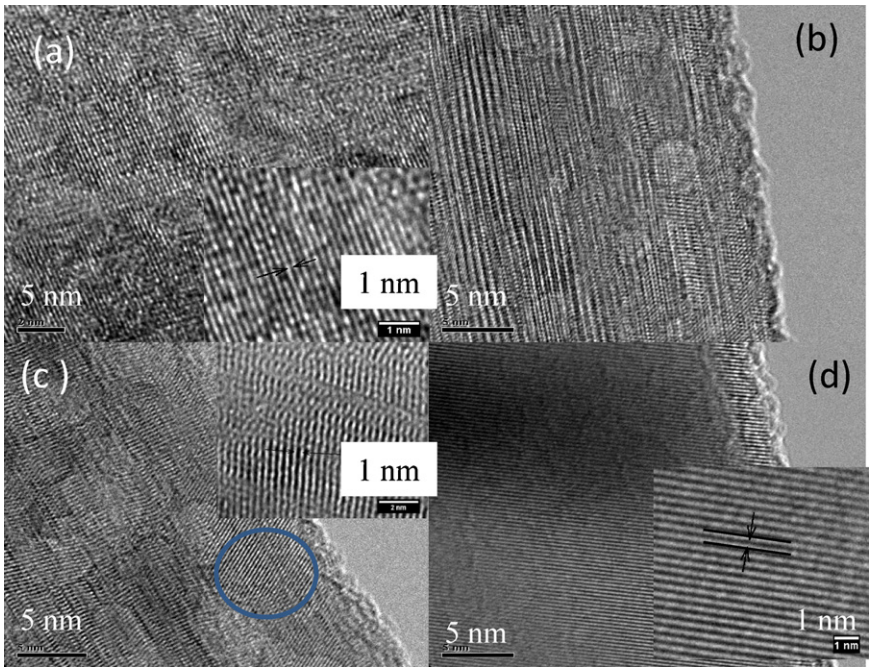

Fig. 4. TEM micrographs of TiO_2 nanowires (a) with washing in water and diluted HCl, and calcined at different temperatures: (b) 400 °C, (c) 500 °C and (d) 700 °C. The inset to (c) corresponds to the area delineated by the circle.

avoid residual Ti fragments inside the membranes, the growth time has been extended to 4 days.

3.3. Porosity characterization

The specific surface area of TiO_2 nanowire membranes is 16.7 m^2/g, which is lower than that of the commercial P25 powder. Fig. 6 presents the UV–NIR absorbance spectra for 250 nm diamond and 50 nm Ag nanoparticle solutions filtered by either two-layer filter paper or TiO_2 membranes, with pure H_2O provided for comparison. The 250 nm diamond particles pass easily through the paper filter, with no remarkable changes in concentration following two filtering passes (data not shown). However, TiO_2 membranes of 0.5 mm thickness removed 95% of the 250 nm diamond particles. The mixture of 50–100 nm nanoparticles with Ag nanowires and some Ag nanobars is clearly observed (Fig. 6, inset). Ag nanowires have a length up to a few micrometers and a diameter of 10 nm, while Ag nanobars have lengths of 100–300 nm and diameters of 20–50 nm. After filtration (Fig. 6(b)), only Ag nanoparticles less than 100 nm and some narrow nanobars (diameter around 20 nm) are present, with long nanowires almost completely removed. In a commensurate reduction, the full-width-half-height (FWHH) of

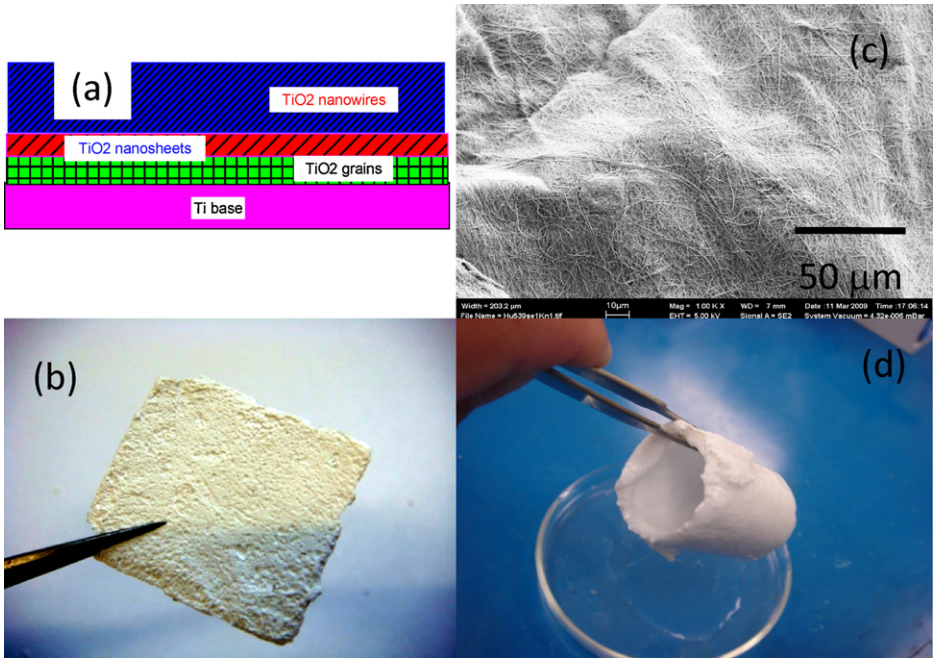

Fig. 5. (a) Schematic diagram for TiO_2 nanowire membranes grown on Ti substrates. (b) A cleaved TiO_2 nanowire membrane. (c) A low resolution image of titanate membranes prior to washing and post-annealing. (d) A tube-shaped TiO_2 nanowire membrane.

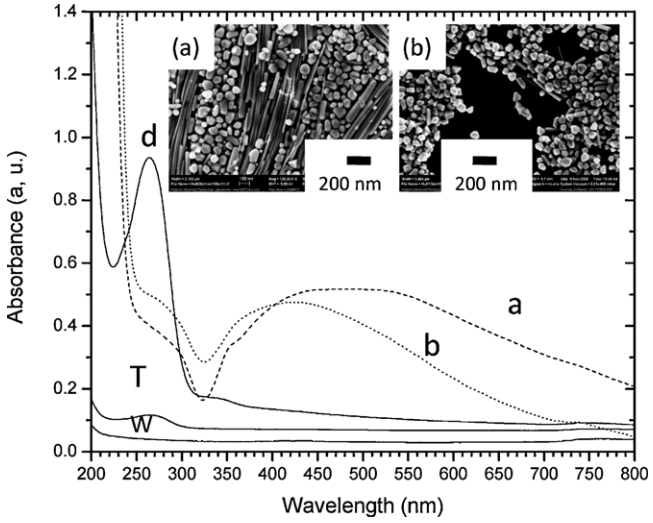

Fig. 6. UV–NIR absorbance spectra of suspended 250 nm diamond colloid solution before (d) and after (T) filtration; and as-grown Ag nanoparticles solution from $AgNO_3$ reduced by sodium citrate before (a) and after (b) filtration relative to pure water (W). Inset: SEM images of (a) As-grown Ag nanoparticles solution, (b) filtered Ag nanoparticles.

absorbance curves became much narrower after membrane filtration relative to that of the as-grown solutions. This indicates that the pore size of TiO_2 membranes is about 100 nm, which is effective for the removal of Ag nanowires. It is important to note that the pore size of TiO_2 membranes is controlled by the membrane thickness and density; the thicker and denser the membrane, the smaller the pore size. However, the present TiO_2 nanowire membranes have low mechanical strength to withstand a high hydraulic pressure, as would be required for any practical filtration application. Additional investigations to produce a carbon fiber composite membrane which would possess enhanced mechanical properties are under way. Besides a requirement to withstand significant hydraulic pressure, any nanofiltration membrane must address biofouling, a notorious issue surrounding any nanofiltration system [33]. Although the ceramic nature of TiO_2 nanowires and effective photocatalytic dissociation can partially mitigate biofouling, further improvements are required prior to the development of a practical TiO_2 nanowire membrane truly resistant to biofouling. With the exception of surface adsorption of contaminants, as described for pharmaceuticals in the following section, the current generation of TiO_2 nanomembranes, while potentially removing bacteria [6,13] does not provide effective ultrafiltration due their pore size.

3.4. Photocatalytic degradation

The diffuse reflectance spectra of titanate nanowires annealed at different temperatures are shown in Fig. 7, with the spectrum of P25 provide for comparison. The absorption margins dramatically increase with annealing temperature, indicating a shrinkage of the energy gap. The optical gap can be estimated from the Tauc plot of $(\alpha h\gamma)^s$ vs. photo energy $h\gamma$ with $s = 0.5$ for an indirect semiconductor [34,35]. From the inset to Fig. 7, the intercepts of the tangents yield 3.30 eV for hydrogen titanate nanowires and 2.9 eV for titanate nanowires annealed at 400–700 °C while for comparison, the commercially available P25 is 3.0 eV. It is well-known that the optical gap is 3.2 eV for anatase [6], 3–3.22 eV for TiO_2-B [36,37], and 3.27 eV for $H_2Ti_3O_7$ nanowires [38]. The slight blue shift of $H_2Ti_3O_7$ nanowires is probably due to the size quantization effect from the remaining $(Na,H)_2Ti_3O_7$ nanosheets [39,40]. On the other hand, the decreasing energy gaps of both TiO_2-B and

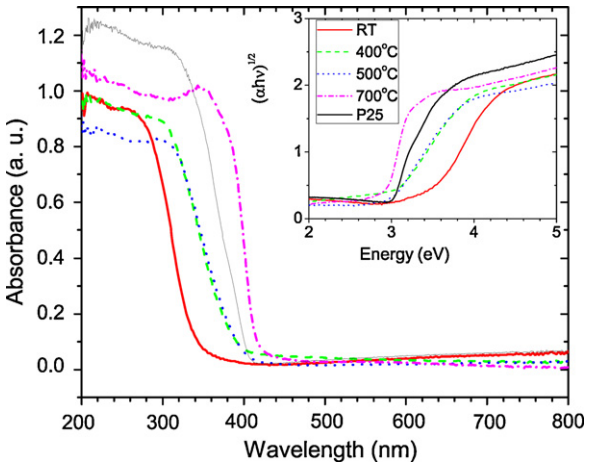

Fig. 7. UV–vis diffuse reflection spectra of TiO_2 membranes with washing in water and diluted HCl and calcined at different temperatures. The spectrum of a commercially available powder, P25, is presented for comparison. Inset: Tauc plot to determine the optical energy gap.

anatase should arise from doping [24,34]; a further investigation on the surface state of nanowires can help to elucidate this issue. Regardless, the current results demonstrate titanate nanowires fabricated through organic solvent-assisted hydrothermal growth have enhanced visual excitation.

The degradation of trimethoprim with TiO_2 nanowire membranes exposed to UV irradiation is illustrated in Fig. 8. A slight decrease in trimethoprim concentration was observed in the presence of UV exposure alone. This may be due to the decomposition of trimethoprim by UV irradiation. However, the decrease in trimethoprim is more pronounced in the presence of the TiO_2 nanowire membranes alone, likely attributable to simple surface adsorption of TiO_2 nanowires as this effect appears saturable as it attenuates rapidly with time. Photocatalytic degradation can be confirmed as the mechanism of trimethoprim removal since there is little change in the concentration of this PPCP in the absence of UV-irradiation of the TiO_2 nanowires. It is notable that TiO_2 nanowire membranes display a better degradation effect than P25

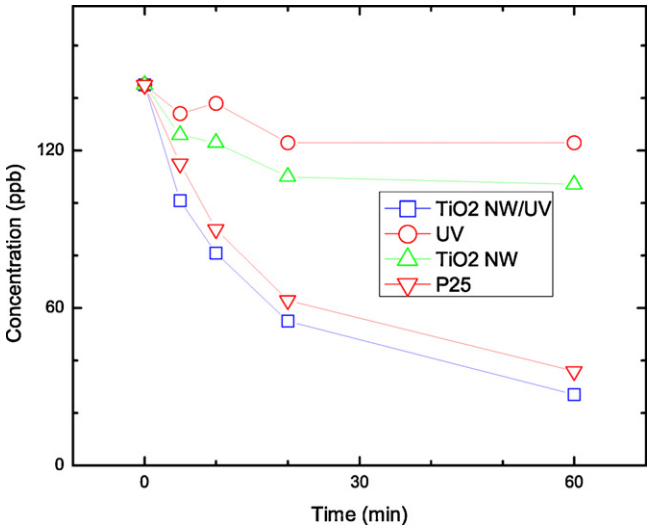

Fig. 8. Concentration of trimethoprim as a function of UV exposure duration only with TiO_2 nanowires membranes(upper triangle), under UV illumination without TiO_2 nanowire membranes (circle), and with TiO_2 nanowire membranes under UV excitation (square). Removal of trimethoprim in the presence of a commercially available powder, P25, with UV exposure is provided for comparison (down triangle).

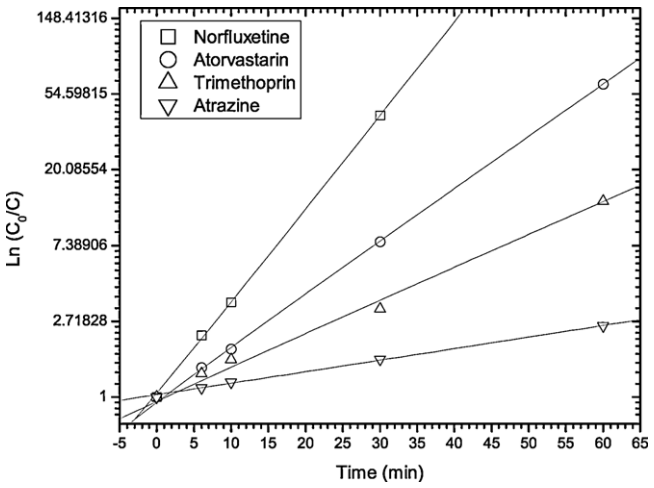

Fig. 9. Kinetic curves of norfluoxetine, atorvastatin, trimethoprim and atrazine degraded by TiO_2 nanowire membranes.

powder. Removal by TiO_2 nanomembranes cannot be attributed to differences in surface area alone as the specific surface area of the commercial P25 powder is actually greater. A possible explanation is that TiO_2 nanowire membranes possess a strong photocatalytic effect. Indeed Fig. 7 displays the enhanced visual excitation of hydrothermal grown TiO_2 nanowires, indicating improved energy harvesting may contribute to the strong photocatalytic effect.

According to previous studies [41–45], the photocatalytic degradation rate of most organic compounds can be described by pseudo-first order kinetics: $-dC/dt = K_{ap}C$, where the C is the concentration and K_{ap} is the apparent reaction rate constant. Integration of the above equation will lead to the concentration as a time function: $\ln(C_0/C) = K_{ap}t$ Using such kinetic analysis, it is evident that the photocatalytic degradation of norfluoxetine, atorvastatin, trimethoprim and atrazine follows the pseudo-first order kinetic (Fig. 9). Notably, similar degradation responses have been observed for other PPCPs and bioactive environmental analytes including fluoxetine, venlafaxin, lincomycin, sulfamethoxazole, diclofenac, bisphenol A, gemfibrozil, carbamazepine and ibuprofen (K_{ap} is given in Table 1). However, a relatively weak degradation effect was observed for carbamazepine and ibuprofen, which are fairly refractory compounds routinely passing through wastewater treatment plants, and consequently often found in surface waters adjacent urban areas [1,3]. However, this data clearly shows that photocatalytic degradation associated with TiO_2 nanowire membranes can effectively remove many PPCP-type pollutants from drinking water. Further investigations on the effects of concentration, temperature, and irradiation intensity are necessary to elucidate the degradation kinetics of pharmaceuticals by TiO_2 nanowire membranes. To evaluate the photocatalytic activities of composite catalysts, it is essential to characterize the extent of mineralization. To identify the intermediate and final species, it is necessary to study the degradation of each pharmaceutical separately, and scan the individual mass spectra of the degradation products. As there are many degradation pathways for these compounds [46,47], comparative studies, currently ongoing, are necessary to fully deduce the mechanisms underlying photocatalytic degradation.

Table 1
Photocatalytic degradation analyzed by the pseudo-first order kinetics for individual pharmaceutical.

Compound	K_{ap}	R^2
Norfluoxetine	0.1239	0.999
Atorvastatin	0.0688	0.999
Lincomycin	0.0430	0.999
Fluoxetine	0.0408	0.995
Venlafaxin	0.0319	0.997
Sulfamethoxazole	0.0422	0.989
Diclofenac	0.0398	0.999
Trimethoprim	0.0269	0.997
Bisphenol A	0.0227	0.988
Gemfibrozil	0.0159	0.993
Atrazine	0.0155	0.999
Carbamazepine	0.0008	0.971
Ibuprofen	0.0005	0.945

4. Conclusions

TiO_2 nanowire membranes can be successfully grown on Ti substrates with hydrothermal processing. Various organic solvents with carbonyl groups provide the oxygen source for initial Ti oxidization. Sodium titanate nanosheets can be fabricated in 10 M NaOH solutions. After washing in water and diluted HCl, sodium titanate can be converted by ion exchange into hydrogen titanate nanowires, which can be further modified into TiO_2-B and anatase phases by calcinations. These phase transitions do not change the morphology of TiO_2 membranes. Collectively, these experiments demonstrate that TiO_2 nanowire membranes can be readily produced with the requisite properties for use in water treatment applications, where their photocatalytic properties can be employed in the degradation of emerging environmental pollutants.

Acknowledgements

This work has been financially supported by the Natural Sciences and Engineering Research Council of Canada, the Canadian Water Network Innovative Technologies for Water Treatment Program, and the Canada Research Chairs Program. X. Zhang would like to thank the Ontario Ministry of Research & Innovation for financial support.

References

[1] C.D. Metcalfe, C.D. Koenig, X.-S. Miao, B.G. Koenig, J. Struger, Distribution of acidic and neutral drugs in surface waters near sewage treatment plants in the lower great lakes, Canada, Environ. Toxicol. Chem. 22 (2003) 2872–2889.
[2] H. Buser, M.E. Balmer, P. Schmid, M. Kohler, Occurrence of UV filters 4-methylbenzylidene camphor and octocrylene in fish from various Swiss rivers with inputs from wastewater treatment plants, Environ. Sci. Technol. 40 (2006) 1427–1431.
[3] M.J. Benotti, B.J. Vanderford, J.C. Holady, B.D. Stanford, S.A. Snyder, Pharmaceuticals and endocrine disrupting compounds in U.S. drinking water, Environ. Sci. Technol. 43 (2009) 597–603.
[4] K. Kummerer, The presence of pharmaceuticals in the environment due to human use—present knowledge and future challenges, J. Environ. Manag. 90 (2009) 2354–2366.
[5] S.A. Snyder, S.A. Adham, A. Redding, F.S. Cannon, J. DeCarolis, J. Oppenheimer, E.C. Wert, Y. Yoon, Role of membranes and activated carbon in the removal of endocrine disruptors and pharmaceuticals, Desalination 202 (2007) 156–181.
[6] X. Zhang, J.H. Pan, A.J. Du, W. Fu, D.D. Sun, J.O. Leckie, Combination of one-dimensional TiO_2 nanowire photocatalytic oxidation with microfiltration for water treatment, Water Res. 43 (2009) 1179–1186.
[7] M.A. Zazouli, H. Susanto, S. Nasseri, M. Ulbricht, Influences of solution chemistry and polymeric natural organic matter on the removal of aquatic pharmaceutical residuals by nanofiltration, Water Res. 43 (2009) 3270–3280.
[8] M. Fujihira, Y. Satoh, T. Osa, Heterogeneous photocatalytic oxidation of aromatic compounds on TiO_2, Nature 293 (1981) 206–208.
[9] A. Liu, Towards development of chemosensors and biosensors with metal-oxide-based nanowires or nanotubes, Biosens. Bioelectron. 24 (2008) 167–177.
[10] X. Chen, S.S. Mao, Titanium dioxide nanomaterials: synthesis, properties, modifications, and applications, Chem. Rev. 107 (2007) 2891–2959.
[11] K. Shankar, J.I. Basham, N.K. Allam, O.K. Varghese, G.K. Mor, X. Feng, M. Paulose, J.A. Seabold, K.-S. Choi, C.A. Grimes, Recent advances in the use of nanotube and nanowire arrays for oxidative photoelectrochemistry, J. Phys. Chem. C 113 (2009) 6327–6359.
[12] W. Dong, A. Cogbill, T. Zhang, S. Ghosh, Z. Ryan Tian, Multifunctional, catalytic nanowire membranes and the membrane-based 3D devices, J. Phys. Chem. B 110 (2006) 16819–16822.

[13] X. Zhang, A.J. Du, P. Lee, D.D. Sun, J.O. Leckie, TiO_2 nanowire membrane for concurrent filtration and photocatalytic oxidation of humic acid in water, J. Membr. Sci. 313 (2008) 44–51.
[14] X. Zhang, T. Zhang, J. Ng, D.D. Sun, High-performance multifunctional TiO_2 nanowire ultrafiltration membrane with a hierarchical layer structure for water treatment, Adv. Funct. Mater. 19 (2009) 3731–3736.
[15] S.P. Albu, A. Ghicov, J.M. Macak, R. Hahn, P. Schmuki, Self-organized, free-standing TiO_2 nanotube membrane for flow-through photocatalytic applications, Nano Lett. 7 (2007) 1286–1289.
[16] T Kasuga, M. Hiramatsu, A. Hoson, T. Sekino, K. Niihara, Formation of titanium oxide nanotube, Langmuir 14 (1998) 3160–3163.
[17] X. Peng, A. Chen, Aligned TiO_2 nanorod arrays synthesized by oxidizing titanium with acetone, J. Mater. Chem. 14 (2004) 2542–2548.
[18] K. Huo, X. Zhang, L. Hu, X. Sun, J. Fu, P.K. Chu, One-step growth and field emission properties of quasialigned TiO_2 nanowire/carbon nanocone core-shell nanostructure arrays on Ti substrates, Appl. Phys. Lett. 93 (2008) 013105-1–013105-3.
[19] H. Wang, Y. Liu, H. Huang, M. Zhong, H. Shen, Hydrothermal growth of large-scale macroporous TiO_2 nanowires and its application in 3D dye-sensitized solar cells, Appl. Phys. A 97 (2009) 25–29.
[20] Y. Wang Y, H. Yang, H. Xu, DNA-like dye-sensitized solar cells based on TiO_2 nanowire-covered nanotube bilayer film electrodes, Mater. Lett. 64 (2010) 164–166.
[21] J.-M. Wu, T.-M. Zhang, Y.-M. Zeng, S. Hayakawa, K. Tsuru, A. Osaka, Large-scale preparation of ordered titania nanorods with enhanced photocatalytic activity, Langmuir 21 (2005) 6995–7002.
[22] Y. Zhao, J. Jin, X. Yang, Hydrothermal synthesis of titanate nanowire arrays, Mater. Lett. 61 (2007) 384–388.
[23] J.E. Boercker, E. Enache-Pommer, E.S. Aydil, Growth mechanism of titanium dioxide nanowires for dye-sensitized solar cells, Nanotechnology 19 (2008) 095604-1–095604-10.
[24] Y. Wu, M. Long, W. Cai, S. Dai, C. Chen, D. Wu, J. Bai, Preparation of photocatalytic anatase nanowire films by in situ oxidation of titanium plate, Nanotechnology 20 (2009) 185703-1–185703-8.
[25] X. Zhang, K. Oakes, S. Cui, L. Bragg, M. Servos, J. Pawliszyn, Tissue-specific in vivo bioaccumulation of pharmaceuticals in rainbow trout (*Oncorhynchus mykiss*) using space-resolved solid-phase microextraction, Environ. Sci. Technol. 44 (2010) 3417–3422.
[26] A.R. Armstrong, G. Armstrong, J. Canales, P.G. Bruce, TiO_2-B nanowires, Angew. Chem. Int. Ed. 43 (2004) 2286–2288.
[27] Y. Suzuki, S. Pavasupree, S. Yoshikawa, Natural rutile-derived titanate nanofibers prepared by direct hydrothermal processing, J. Mater. Res. 20 (2005) 1063–1070.
[28] M. Wei, K. Wei, M. Ichihara, H. Zhou, High rate performances of hydrogen titanate nanowires electrodes, Electrochem. Commun. 10 (2008) 1164–1167.
[29] B. Zhao, F. Chen, W. Qu, J. Zhang, The evolvement of pits and dislocations on TiO_2-B nanowires via oriented attachment growth, J. Soild State Chem. 182 (2009) 2225–2230.
[30] Y.X. Zhang, G.H. Li, Y.X. Jin, Y. Zhang, J. Zhang, L.D. Zhang, Hydrothermal synthesis and photoluminescence of TiO_2 nanowires, Chem. Phys. Lett. 365 (2002) 300–304.
[31] R.L. Penn, J.F. Banfield, Imperfect oriented attachment: dislocation generation in defect-free nanocrystals, Science 281 (1998) 969–971.
[32] M. Wei, Y. Konishi, H. Zhou, H. Sugihara, H. Arakawa, A simple method to synthesize nanowires titanium dioxide from layered titanate particles, Chem. Phys. Lett. 400 (2004) 231–234.
[33] F. Dong, W. Zhao, Z. Wu, Characterization and photocatalytic activities of C, N and S co-doped TiO_2 with 1D nanostructure prepared by the nano-confinement effect, Nanotechnology 19 (2008) 36507-1–36507-10.
[34] Z. Wu, F. Dong, W. Zhao, H. Wang, Y. Liu, B. Guan, The fabrication and characterization of novel carbon doped TiO_2 nanotubes, nanowires, and nanorods with high visible light photocatalytic activity, Nanotechnology 20 (2009) 235701-1–235701-9.
[35] S Yin, J. Wu, M. Aki, T. Sato, Photocatalytic hydrogen evolution with fibrous titania prepared by the solvothermal reactions of protonic layered tetratitanate ($H_2Ti_4O_9$), Int. J. Inorg. Mater. 2 (2000) 325–331.
[36] J. Prochazka, L. Kavan, M. Zukalova, O. Frank, M. Kalbac, A. Zukal, M. Klementova, D. Carbone, M. Graetzel, Novel synthesis of the TiO_2 (B) multilayer template films, Chem. Mater. 21 (2009) 1457–1464.
[37] Y. Kim II, S.J. Atherton, E.S. Brigham, T.E. Mallouk, Sensitized layered metal oxide semiconductor particles for photochemical hydrogen evolution from nonsacrificial electron donors, J. Phys. Chem. 97 (1993) 11802–11810.
[38] T. Sasaki, M. Watanabe, Semiconductor nanosheet crystallines of quasi-TiO_2 and their optical properties, J. Phys. Chem. B 101 (1997) 10159–10161.
[39] N. Sakai, Y. Ebina, K. Takada, T. Sasaki, Electronic band structure of titania semiconductor nanosheets revealed by electrochemical and photoelectrochemical studies, J. Am. Chem. Soc. 126 (2004) 5851–5858.
[40] B. Van der Bruggen, M. Manttari, M. Nystrom, Drawbacks of applying nanofiltration and how to avoid them: a review, Sep. Purif. Technol. 62 (2008) 251–263.
[41] M.A. Rauf, S. Salman Ashraf, Fundamental principles and application of heterogeneous photocatalytic degradation of dyes in solution, Chem. Eng. J. 151 (2009) 10–18.
[42] I. Bouzaida, C. Ferronato, J.M. Chovelon, M.E. Rammah, J.M. Herrmann, Heterogeneous photocatalytic degradation of the anthraquinonic dye, Acid Blue 25: a kinetic approach, J. Photochem. Photobiol. 168 (2004) 23–30.
[43] N. Barka, S. Qourzal, A. Nounah, Y. Ait-Ichou, Factors influencing the photocatalytic degradation of Rhodamine B by TiO_2-coated non-woven paper, J. Photochem. Photobiol. A 195 (2008) 346–351.
[44] Y. Liu, J. Li, B. Zhou, J. Bai, Q. Zheng, J. Zhang, W. Cai, Comparison of photoelectrochemical properties of TiO_2-nanotube-array photoanode prepared by anodization in different electrolyte, Environ. Chem. Lett. 7 (2008) 363–368.
[45] Y. Liu, X. Gan, B. Zhou, B. Xiong, J. Li, C. Dong, J. Bai, W. Cai, Photoelectrocatalytic degradation of tetracycline by highly effective TiO_2 nanopore arrays electrode, J. Hazard. Mater. 171 (2009) 678–683.
[46] F. Mendez-Arriaga, S. Esplugas, J. Gimenez, Photocatalytic degradation of non-steroidal anti-inflammatory drugs with TiO_2 and simulated solar irradiation, Water Res. 42 (2008) 585–594.
[47] P. Calza, C. Massolino, G. Monaco, C. Medana, C. Baiocchi, Study of the photocatalytic transformation of amiloride in water, J. Pharm. Biomed. Anal. 48 (2008) 315–320.